

A Positive Flux Limited Difference Scheme for Option Pricing 2D Fully Non-linear Parabolic Equation with Uncertain Correlation

Miglena N. Koleva, Lubin G. Vulkov

University of Rousse , 8 Studentska St., 7017 Rousse, Bulgaria
{mkoleva,lwalkov}@uni-ruse.bg

Abstract

We consider a two-asset non-linear model of option pricing in an environment where the correlation is not known precisely, as it varies between two known values. First we discuss the non-negativity of the solution of the problem. Next, we construct and analyze a positivity preserving, flux-limited finite difference scheme for the corresponding boundary value problem. Numerical experiments are analyzed.

Keywords. Two-asset worst-case option pricing model, fully non-linear parabolic equation, positive ODE system, van Leer flux-limiter, non-negativity preservation, stability

1 Introduction

Very important for the valuation of option pricing models is the correct specification of the respective model parameters. Some of them are given from the market, or estimated from historic or forward looking data but others are the result of calibration to market prices. These techniques leads to more realistic in practice *non-linear* models with uncertain parameter values, for example volatility, interest rate, dividend or correlation.

Usually this parameters range between upper and lower known bounds and consequently we may consider highest and lowest option value, called *best* and *worst* values. These prices can be interpret as *worst-case pricing* for short and long position respectively.

Well-known one-factor uncertain volatility models are derived by Avellaneda, Levy and Parás [1]. Following Black-Scholes hedging and no-arbitrage arguments they construct a worst/best option pricing model where the value of the volatility depends on the sign of the second derivative, the Gamma greek (Γ).

The same idea applied to the case of uncertain interest rate or uncertain dividend yield (independent of the asset price) in the case of continuous dividend leads to non-linear one-asset uncertain parameter models, which gives a consistent way to eliminate the dependence of a price on a parameter and to some extent reduce model dependence [27].

The same arguments [27, p.313] can be carried over to multi-asset models, strongly dependent on the correlation ρ between the stochastic processes of the underlying state variable. The correlation is difficult to guess or calculate in practice so it can be considered as uncertainty. Following [2] and [27], this simple hedging strategy is realized in [22] for two-asset

option pricing model. To be self-contained we outline the derivation of the model, presented in [22].

Consider the correlation bounded by $-1 \leq \rho_1 \leq \rho \leq \rho_2 \leq 1$ and define the price movements of two underlying assets S_1, S_2 (for time t , trends (drift rates) μ_1, μ_2 , volatilities σ_1, σ_2 and increments of standard Wiener's process dX)

$$\begin{aligned} dS_1 &= \mu_1 S_1 dt + \sigma_1 S_1 dX, \\ dS_2 &= \mu_2 S_2 dt + \sigma_2 S_2 dX, \end{aligned}$$

correlated by $E(dX_i dX_j) = \rho dt$.

By Itô's Lemma we express an infinitesimal change in the portfolio (Π), consisting of a long position in one option and short position in both underlyings. Next, eliminating the risk, just as in the classical argument when deriving the Black-Scholes equation for the option price $V(S_1, S_2, t)$ we get

$$d\Pi = \left(\frac{\partial V}{\partial t} + \frac{1}{2} \sigma_1^2 S_1^2 \frac{\partial^2 V}{\partial S_1^2} + \frac{1}{2} \sigma_2^2 S_2^2 \frac{\partial^2 V}{\partial S_2^2} + \rho \sigma_1 \sigma_2 S_1 S_2 \frac{\partial^2 V}{\partial S_1 \partial S_2} \right) dt.$$

In order to derive worst-case scenario model we will be extremely pessimistic: in every infinitesimal time step we assume that a correlation leads to the smallest growth in the portfolio, i.e.

$$\min_{\rho} d\Pi = r\Pi dt, \quad \text{where } r > 0 \text{ is the interest rate.} \quad (1)$$

Taking into account that the portfolio consists of a long position in one option and short position in both underlying we have

$$r\Pi dt = r \left(V(S_1, S_2, t) - \frac{\partial V}{\partial S_1} S_1 - \frac{\partial V}{\partial S_2} S_2 \right) dt \quad (2)$$

and

$$\begin{aligned} \min_{\rho} d\Pi &= \min_{\rho} \left\{ \left(\frac{\partial V}{\partial t} + \frac{1}{2} \sigma_1^2 S_1^2 \frac{\partial^2 V}{\partial S_1^2} + \frac{1}{2} \sigma_2^2 S_2^2 \frac{\partial^2 V}{\partial S_2^2} + \rho \sigma_1 \sigma_2 S_1 S_2 \frac{\partial^2 V}{\partial S_1 \partial S_2} \right) dt \right\} \\ &= \begin{cases} \frac{\partial V}{\partial t} + \frac{1}{2} \sigma_1^2 S_1^2 \frac{\partial^2 V}{\partial S_1^2} + \frac{1}{2} \sigma_2^2 S_2^2 \frac{\partial^2 V}{\partial S_2^2} + \rho_1 \sigma_1 \sigma_2 S_1 S_2 \frac{\partial^2 V}{\partial S_1 \partial S_2}, & \frac{\partial^2 V}{\partial S_1 \partial S_2} > 0, \\ \frac{\partial V}{\partial t} + \frac{1}{2} \sigma_1^2 S_1^2 \frac{\partial^2 V}{\partial S_1^2} + \frac{1}{2} \sigma_2^2 S_2^2 \frac{\partial^2 V}{\partial S_2^2} + \rho_2 \sigma_1 \sigma_2 S_1 S_2 \frac{\partial^2 V}{\partial S_1 \partial S_2}, & \frac{\partial^2 V}{\partial S_1 \partial S_2} < 0. \end{cases} \end{aligned} \quad (3)$$

Combining (2), (3) via (1) and taking into account the dividends (denoted by D_1 and D_2) we obtain the worst-case pricing equation

$$\begin{aligned} \frac{\partial V}{\partial t} + \frac{1}{2} \sigma_1^2 S_1^2 \frac{\partial^2 V}{\partial S_1^2} + \frac{1}{2} \sigma_2^2 S_2^2 \frac{\partial^2 V}{\partial S_2^2} + \rho(\Gamma_{cross}) \sigma_1 \sigma_2 S_1 S_2 \frac{\partial^2 V}{\partial S_1 \partial S_2} \\ + (r - D_1) S_1 \frac{\partial V}{\partial S_1} + (r - D_2) S_2 \frac{\partial V}{\partial S_2} - rV = 0, \quad (S_1, S_2) \in \Omega = \mathbb{R}^+ \times \mathbb{R}^+, \quad 0 \leq t < T; \end{aligned} \quad (4)$$

$$\rho(\Gamma_{cross}) = \begin{cases} \rho_1, & \Gamma_{cross} > 0, \\ \rho_2, & \Gamma_{cross} < 0. \end{cases}, \quad \Gamma_{cross} = \frac{\partial^2 V}{\partial S_1 \partial S_2}, \quad -1 \leq \rho_1 \leq \rho_2 \leq 1. \quad (5)$$

In the best-case scenario for an investor with long position, $\rho(\Gamma_{cross})$ is determined by

$$\rho(\Gamma_{cross}) = \begin{cases} \rho_1, & \Gamma_{cross} < 0, \\ \rho_2, & \Gamma_{cross} > 0. \end{cases}$$

There are many numerical methods for one-asset uncertain parameter models available in the literature. For example, for the uncertain volatility model (which is identical with Leland model of transaction cost [27]), in [17] is developed numerical iteration algorithm. Positivity preserving method is presented in [12]. A fully-implicit, monotone discretization method is developed for the solution of option pricing model with uncertain drift rate in [28].

For multi-asset (or two-asset) *linear models*, various numerical methods can be found in the literature, e.g. [3], where the authors present positivity preserving numerical approach for two-asset linear option pricing stochastic volatility model.

Amid numerous publications, related to the numerical solution of option pricing models, the investigations concerning non-linear multi-asset option pricing models are scarce. The only work (we managed to find in the literature), related to the non-linear two-asset option pricing model with uncertain correlation, is the paper of J. Topper [22]. The author implement the collocation finite element method with cubic Hermite trial functions to solve the worst-case scenario for the considered problem.

In [16] a two-asset stochastic correlation model is considered, where the correlation coefficient is a random walk following the square root process. This leads to linear model that is solved by quasi-Monte Carlo method.

In this paper we develop a second-order positivity preserving numerical method for the problem (4),(5). We construct implicit-explicit difference scheme, using different stencils, in dependence of the sign of correlation, for the approximation of Γ_{cross} and application of van Leer flux limiter approach for the first derivative discretization. Mild restrictions for space and time mesh step sizes guarantee the stability and *positivity preserving property* of the numerical solution, i.e. starting with non-negative initial data to obtain a non-negative numerical solution at each time layer.

The rest of the paper is organized as follows. In the next section, we formulate the differential problem on bounded domain, after application of the exponential variable change [4, 25]. The non-negativity of the solution is discussed. Combining the monotone techniques in [18, 20] with flux limiting, we perform a space discretization of the problem in Section 3. A positive fully-discrete scheme is derived in the next section. Numerical results are discussed in Section 5 and the paper is completed by some conclusions.

2 The differential problem

Let now $\bar{\Omega} = \Omega \cup \partial\Omega = [L_W, L_E] \times [L_S, L_N] \subseteq \mathbb{R}^+ \times \mathbb{R}^+$. Following the financial modelling in [22] we consider the equation (4), (5), associated with the terminal and boundary conditions [21, 22, 23, 24]

$$V(S_1, S_2, T) = g_0(S_1, S_2) \geq 0 \text{ in } \Omega \tag{6}$$

$$\frac{\partial V(S_1, S_2, t)}{\partial n} = g_1(S_1, S_2, t) \geq 0 \text{ on } \partial\Omega_1, \tag{7}$$

$$V(S_1, S_2, t) = g_2(S_1, S_2, t) \geq 0 \text{ on } \partial\Omega_2 \neq \emptyset, \quad \partial\Omega_1 \cup \partial\Omega_2 = \partial\Omega. \tag{8}$$

Here $\partial/\partial n$ is the outward derivative to S_1 or S_2 and T is time to maturity.
Using the logarithmic prices

$$x_i = \ln S_i, \quad i = 1, 2, \quad \tau = T - t, \quad (9)$$

we introduce the operators

$$\begin{aligned} \mathcal{L}_i u &= -\frac{1}{2}\sigma_1^2 \frac{\partial^2 u}{\partial x_1^2} - \frac{1}{2}\sigma_2^2 \frac{\partial^2 u}{\partial x_2^2} - \rho_i \sigma_1 \sigma_2 \frac{\partial^2 u}{\partial x_1 \partial x_2} \\ &\quad - (r - D_1 - \frac{1}{2}\sigma_1^2) \frac{\partial u}{\partial x_1} - (r - D_2 - \frac{1}{2}\sigma_2^2) \frac{\partial u}{\partial x_2} + ru, \quad i = \{0, 1, 2\}, \end{aligned}$$

where we formally set $\rho_0 = \rho(\tilde{\Gamma}'_{cross})$. Then (4)-(8) is transformed to the following problem for $u(x_1, x_2, \tau) = V(S_1, S_2, t)$, $(x_1, x_2) \in \overline{\Omega'} = [\ln L_W, \ln L_E] \times [\ln L_S, \ln L_N] \subseteq \mathbb{R}^2$.

$$\frac{\partial u}{\partial \tau} + \mathcal{L}_0 u = 0, \quad (x_1, x_2, \tau) \in Q_T \equiv \Omega' \times (0, T); \quad (10)$$

$$\Gamma'_{cross} = e^{-(x_1+x_2)} \frac{\partial^2 u}{\partial x_1 \partial x_2}, \quad \tilde{\Gamma}'_{cross} = \frac{\partial^2 u}{\partial x_1 \partial x_2}, \quad (11)$$

$$u(x_1, x_2, 0) = g'_0(x_1, x_2) \text{ in } \Omega' \quad (12)$$

$$\frac{\partial u(x_1, x_2, \tau)}{\partial n'} = g'_1(x_1, x_2, \tau) \text{ on } \partial\Omega'_1, \quad (13)$$

$$u(x_1, x_2, \tau) = g'_2(x_1, x_2, \tau) \text{ on } \partial\Omega'_2, \quad \partial\Omega'_1 \cup \partial\Omega'_2 = \partial\Omega', \quad (14)$$

where $\partial/\partial n'$ is the outward derivative to x_1 or x_2 , $g'_0(x_1, x_2) = g_0(e^{x_1}, e^{x_2})$, $g'_2(x_1, x_2, \tau) = g_2(e^{x_1}, e^{x_2}, \tau)$ and

$$g'_1(x_1, x_2, \tau) = \begin{cases} e^{x_1} g_1(e^{x_1}, e^{x_2}, \tau), & x_1 = \ln L_W \text{ or } x_1 = \ln L_E, \\ e^{x_2} g_1(e^{x_1}, e^{x_2}, \tau), & x_2 = \ln L_S \text{ or } x_2 = \ln L_N. \end{cases}$$

The notation $(\cdot)'$ indicates the transformed by (9) object (\cdot) .

Due to the complexity of the presented nonlinear model there are difficulties in obtaining existence and uniqueness results for problem (10)-(14). In this paper we are not concerned with this aspect of the problem but we shall discuss the minimum principle.

We denote by $C^{m,q}(Q_T)$ the space of functions defined on Q_T that have continuous derivative with respect to $x = (x_1, x_2)$ up to order m and continuous derivative with respect to t up to order q .

Typically, no $C^{2,1}$ solution exists on the hole domain Q_T of equation (10) with discontinuous function ρ_0 . The particularity of the equation (10) is that it shows degeneracy, because it is possible $\tilde{\Gamma}'_{cross} = 0$. Thus it is naturally to assume the existence of a set $\mathcal{S}(x_1, x_2, \tau) \subset Q_T$ on which $\tilde{\Gamma}'_{cross}(x_1, x_2, \tau) = 0$. This set (it is expected to be a surface) is not given in advance so that we have a Stefan-like problem. But (10) is derived from stochastic finance and therefore specific interface (internal boundary) conditions are needed. We assume $u \in C^{2,1}(Q_T)$ across the phase-change surfaces that is in accordance with condition $\tilde{\Gamma}'_{cross}(x_1, x_2, \tau)|_{\mathcal{S}} = 0$. Out of the interface $\mathcal{S}(x_1, x_2, \tau)$ we assume even higher regularity, $u \in C^{3,1}(\Omega_T \setminus \mathcal{S})$. By $\partial\Omega_T^p$ we denote the parabolic boundary of $\overline{Q_T}$, i.e. $\partial\Omega_T^p = \{(x_1, x_2, \tau) : (x_1, x_2) \in \partial\Omega', 0 \leq \tau < T\}$, i.e. the boundary of Q_T minus the interior of the top part of the boundary, $\Omega' \times \{\tau = T\}$. Also, by Q_T^+ (Q_T^-) we will denote the subset of Q_T , where $\tilde{\Gamma}'_{cross} > 0$ ($\tilde{\Gamma}'_{cross} < 0$).

Theorem 1 (Minimum Principle) *Suppose that the function $u \in C(\overline{Q_T}) \cap C^{2,1}(Q_T) \cap C^{3,1}(\Omega_T \setminus \mathcal{S})$ satisfies in Q_T the problem (10)-(14) and $g'_0(x_1, x_2) \geq 0$ in Ω' and $g'_i(x_1, x_2, \tau) \geq 0$ on $\partial\Omega'_i$, $i = 1, 2$. Then u can not attain negative local minimum in $\overline{Q_T} \setminus \partial Q_T^p$ and $u \geq 0$ on $\overline{Q_T}$.*

Proof. Suppose that there exists a local minimum point $P_0(x_{1_0}, x_{2_0}, \tau_0) \in Q_T$ with $u(P_0) < 0$.

1. If $0 < \tau_0 < T$, then P_0 belongs to the interior of Q_T and therefore,

$$\frac{\partial u}{\partial \tau}(P_0) = \frac{\partial u}{\partial x_1}(P_0) = \frac{\partial u}{\partial x_2}(P_0) = 0, \quad (15)$$

and

$$\frac{\partial^2 u}{\partial x_1^2}(P_0) \geq 0, \quad \frac{\partial^2 u}{\partial x_2^2}(P_0) \geq 0. \quad (16)$$

1.1. Suppose $P_0 \in S$. Then $\frac{\partial^2 u}{\partial x_1 \partial x_2} = 0$ and (15), (16) lead to

$$\left(\frac{\partial u}{\partial \tau} + \mathcal{L}_0 u \right) (P_0) < 0,$$

which contradicts to equation (10).

1.2. Suppose that $P_0 \in Q_T^+$ (similar is the treatment of the case $P_0 \in Q_T^-$). Then, in view of (15), (16) we have

$$\begin{aligned} 0 &= \left(\frac{\partial u}{\partial \tau} + \mathcal{L}_1 u \right) (P_0) = \mathcal{L}_1 u(P_0) \\ &= -\frac{1}{2}\sigma_1^2 \frac{\partial^2 u}{\partial x_1^2}(P_0) - \frac{1}{2}\sigma_2^2 \frac{\partial^2 u}{\partial x_2^2}(P_0) - \rho_1 \sigma_1 \sigma_2 \frac{\partial^2 u}{\partial x_1 \partial x_2}(P_0) + ru(P_0). \end{aligned} \quad (17)$$

Since P_0 is not on the boundary of Q_T , there is a neighborhood of (x_{1_0}, x_{2_0}, t_0) within of the domain Q_T where we can use the Taylor expansion:

$$\begin{aligned} u(x_{1_0} + \Delta x_1, x_{2_0} + \Delta x_2, \tau_0) &= u(P_0) \\ &+ \frac{1}{2} \left(\frac{\partial^2 u}{\partial x_1^2}(P_0)(\Delta x_1)^2 + 2\Delta x_1 \Delta x_2 \frac{\partial^2 u}{\partial x_1 \partial x_2}(P_0) + \frac{\partial^2 u}{\partial x_2^2}(P_0)(\Delta x_2)^2 \right) + O((\Delta x_1)^3 + (\Delta x_2)^3). \end{aligned}$$

Taking into account that $u(x_{1_0} + \Delta x_1, x_{2_0} + \Delta x_2, \tau_0) > u(P_0)$ for all Δx_1 and Δx_2 that are small enough, we have

$$\frac{\partial^2 u}{\partial x_1^2}(P_0)(\Delta x_1)^2 + 2\Delta x_1 \Delta x_2 \frac{\partial^2 u}{\partial x_1 \partial x_2}(P_0) + \frac{\partial^2 u}{\partial x_2^2}(P_0)(\Delta x_2)^2 \geq 0. \quad (18)$$

Since $u(P_0) < 0$, from (17) follows that

$$\sigma_1^2 \frac{\partial^2 u}{\partial x_1^2}(P_0) + 2\rho_1 \sigma_1 \sigma_2 \frac{\partial^2 u}{\partial x_1 \partial x_2}(P_0) + \sigma_2^2 \frac{\partial^2 u}{\partial x_2^2}(P_0) < 0. \quad (19)$$

In order to match the Taylor expansion to get a contradiction, we require the last inequality as

$$\left(\frac{\sigma_1}{\sqrt{C}} \right)^2 \frac{\partial^2 u}{\partial x_1^2}(P_0) + 2\rho_1 \frac{\sigma_1}{\sqrt{C}} \frac{\sigma_2}{\sqrt{C}} \frac{\partial^2 u}{\partial x_1 \partial x_2}(P_0) + \left(\frac{\sigma_2}{\sqrt{C}} \right)^2 \frac{\partial^2 u}{\partial x_2^2}(P_0) < 0, \quad (20)$$

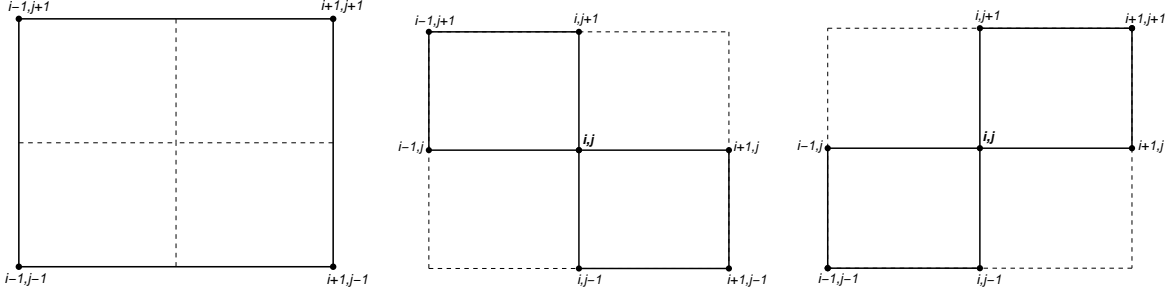


Figure 1: Stencils, corresponding to $u_{\hat{x}_1\hat{x}_2i,j}$ (left), $u_{x_1x_2i,j}^-$ (center) and $u_{x_1x_2i,j}^+$ (right)

where $C > 0$ is a constant. Next we take

$$\Delta x_1 = \frac{\sigma_1}{\sqrt{C}} \quad \text{and} \quad \Delta x_2 = \frac{\sigma_2}{\sqrt{C}}.$$

This contradicts to (19) for sufficiently large C .

1.3. Suppose $P_0 \in \partial\Omega'_1$ and for concreteness let $P_0(\ln L_W, x_2, \tau)$, i.e. $x_{10} = \ln L_W$. Then following similar considerations as in the Hopf's lemma [5], we conclude that $\partial u / \partial n(P_0) > 0$, where $n(P_0)$ is the outer normal. But $\partial u / \partial n(P_0) = -\partial u / \partial x(P_0) = g_1(P_0) \leq 0$, so we get contradiction.

2. Now suppose $\tau_0 = T$. Then we will have $\frac{\partial u}{\partial \tau}(P_0) \leq 0$, instead of $\frac{\partial u}{\partial \tau}(P_0) = 0$ in (15) and we once more deduce the contradiction in the cases 1.1, 1.2 and 1.3. \square

3 Space discretization

In the present section we develop the numerical method, combining the idea of A. Samarskii et al. [20] to use different stencils for the approximation of the mixed derivative with the flux limiter approach [6, 10, 15] in two space directions for approximation of the first derivatives.

We define an uniform mesh in space $\bar{\Omega}$

$$\begin{aligned} \bar{\omega}_h &= \{x = (x_{1i}, x_{2j}) : x_{1i} = L_W + (i-1)h_1, \quad x_{2j} = L_S + (j-1)h_2, \\ i &= 1, \dots, N_1, \quad j = 1, \dots, N_2, \quad h_1 = (L_W - L_E)/(N_1 - 1), \quad h_2 = (L_N - L_S)/(N_2 - 1)\} \end{aligned}$$

and denote the numerical solution at point (x_{1i}, x_{2j}, τ) by $u_{i,j}(\tau) := u(x_{1i}, x_{2j}, \tau)$.

Further, we use the notations

$$\begin{aligned} u_{\bar{x}_{1i,j}} &= \frac{u_{i,j} - u_{i-1,j}}{h_1}, \quad u_{x_{1i,j}} = u_{\bar{x}_{1i+1,j}}, \quad u_{\bar{x}_{2i,j}} = \frac{u_{i,j} - u_{i,j-1}}{h_2}, \quad u_{x_{2i,j}} = u_{\bar{x}_{2i,j+1}}, \\ u_{\hat{x}_{s_i,j}} &= \frac{1}{2}[u_{x_{s_i,j}} + u_{\bar{x}_{s_i,j}}], \quad u_{\bar{x}_s x_p} = (u_{\bar{x}_s})_{x_p}, \quad u_{\hat{x}_s \hat{x}_p} = (u_{\hat{x}_s})_{\hat{x}_p}, \quad s, p \in \mathbb{N}, \\ u_{x_1 x_2 i,j}^- &= \frac{1}{2}[u_{\bar{x}_1 x_2 i,j} + u_{x_1 \bar{x}_2 i,j}], \quad u_{x_1 x_2 i,j}^+ = \frac{1}{2}[u_{x_1 x_2 i,j} + u_{\bar{x}_1 \bar{x}_2 i,j}], \quad \text{see Figure 1.} \end{aligned}$$

We may present an arbitrary function v in the form $v = v^+ - v^-$ (and $|v| = v^+ + v^-$), where $v^+ = \max\{0, v\}$ and $v^- = \max\{0, -v\}$. Thus, according to (5) and (11) for $\rho'_{i,j} := \rho(\bar{\Gamma}'_{cross_{i,j}})$

we have

$$\rho'_{i,j} = \rho'_{i,j}{}^+ - \rho'_{i,j}{}^- = \begin{cases} \rho_1^+ - \rho_1^-, & \tilde{\Gamma}'_{crossi,j} > 0, \\ \rho_2^+ - \rho_2^-, & \tilde{\Gamma}'_{crossi,j} < 0. \end{cases} \quad (21)$$

For approximation of the first derivatives in (10) we apply van Leer flux limiter technique [6, 10, 15] in both space directions. Consider the conservative derivatives approximation

$$\begin{aligned} A_s \frac{\partial u}{\partial x_s} &= A_s \frac{\partial u}{\partial x_s} \simeq A_s \frac{U_{e_s+1/2} - U_{e_s-1/2}}{h_s}, \quad s = \{1, 2\}, \quad \text{where} \\ A_s &= r - D_s - \frac{1}{2}\sigma_s^2, \quad U_{e_s \pm q} = \begin{cases} u_{i \pm q, j}, & s = 1, \\ u_{i, j \pm q}, & s = 2, \end{cases} \quad q \in \mathbb{R}. \end{aligned} \quad (22)$$

Using gradient ratios

$$\theta_{e_s+1/2} = \frac{u_{x_{s i, j}}}{u_{\bar{x}_{s i, j}}}, \quad (23)$$

we define van Leer flux limiter [6, 10, 14]

$$\Phi(\theta) = \frac{|\theta| + \theta}{1 + |\theta|}. \quad (24)$$

Observe that $\Phi(\theta)$ is Lipschitz continuous, continuously differentiable for all $\theta \neq 0$, and

$$\Phi(\theta) = 0, \quad \text{if } \theta \leq 0 \quad \text{and} \quad \Phi(\theta) \leq 2 \min\{1, \theta\}. \quad (25)$$

Note that at the extreme points of u , the slopes $u_{x_{s i, j}}$ and $u_{\bar{x}_{s i, j}}$ have opposite signs and $\Phi(\theta_{e_s+1/2}) = 0$.

Following [6] the numerical flux $U_{e_s+1/2}$ is approximated in a non-linear way

$$U_{e_s+1/2} = U_{e_s} + \frac{1}{2}\Phi(\theta_{e_s+1/2})(U_{e_s} - U_{e_s-1}). \quad (26)$$

Reflecting the indices that appear in $u_{i,j}$ about $i + 1/2$ or $j + 1/2$ yields [6]

$$U_{e_s+1/2} = U_{e_s+1} + \frac{1}{2}\Phi(\theta_{e_s+3/2}^{-1})(U_{e_s+1} - U_{e_s+2}). \quad (27)$$

Similarly, the flux $U_{e_s-1/2}$, corresponding to (26) and (27) is defined by shifting the index s (i.e. i or j).

Using the symmetry property of the flux limiter $\Phi(\theta) = \theta\Phi(\theta^{-1})$ [13] and (23), we approximate $A_s \frac{\partial u}{\partial x_s}$ at point (x_{1i}, x_{2j}, τ) , applying (26) and (27) in dependence of the sign of $A_s = A_s^+ - A_s^-$:

$$\begin{aligned} A_s \frac{\partial u}{\partial x_s} &\simeq A_s^+ \Lambda_s^+ u_{x_s} - A_s^- \Lambda_s^- u_{\bar{x}_s}, \quad s = \{1, 2\}, \\ \Lambda_s^+ &= 1 + \frac{1}{2}\Phi(\theta_{e_s+1/2}^{-1}) - \frac{1}{2}\Phi(\theta_{e_s+3/2}), \quad \Lambda_s^- = 1 + \frac{1}{2}\Phi(\theta_{e_s+1/2}) - \frac{1}{2}\Phi(\theta_{e_s-1/2}^{-1}), \end{aligned} \quad (28)$$

where $0 \leq \Lambda_s^- \leq 2$ and $0 \leq \Lambda_s^+ \leq 2$ in view of (24), (25).

We implement the idea of [18] so that we use different stencils for the approximation of the second mixed derivative and by (28), we obtain the following discretization for (10) at point (x_{1i}, x_{2j}, τ) , $2 < i < N_1 - 1$, $2 < j < N_2 - 1$:

$$\begin{aligned} \frac{\partial u}{\partial \tau} - \frac{1}{2}\sigma_1^2 u_{\bar{x}_1 x_1} - \frac{1}{2}\sigma_2^2 u_{\bar{x}_2 x_2} - \sigma_1 \sigma_2 (\rho'^+ u_{x_1 x_2}^+ - \rho'^- u_{x_1 x_2}^-) \\ - A_1^+ \Lambda_1^+ u_{x_1} + A_1^- \Lambda_1^- u_{\bar{x}_1} - A_2^+ \Lambda_2^+ u_{x_2} + A_2^- \Lambda_2^- u_{\bar{x}_2} + ru = 0, \end{aligned} \quad (29)$$

where $\tilde{\Gamma}'_{cross_{i,j}} \simeq u_{\hat{x}_s \hat{x}_p}_{i,j}$ and $\rho'_{i,j} = \rho'(u_{\hat{x}_s \hat{x}_p}_{i,j})$.

For computing the gradient ratio in grid points for $i = \{2, N_1 - 1\}$ or $j = \{2, N_2 - 1\}$ we need the values of $u_{i,j}$ at the outer grid nodes (x_{10}, x_{2j}, τ) , $(x_{1N_1+1}, x_{2j}, \tau)$, (x_{1i}, x_{20}, τ) and $(x_{1i}, x_{2N_2+1}, \tau)$ for $1 < i < N_1$, $1 < j < N_2$. Then the second-order extrapolation formulas [19] will be used

$$\begin{aligned} u_{0,j} = 3u_{1,j} - 3u_{2,j} + u_{3,j}, \quad u_{N_1+1,j} = 3u_{N_1,j} - 3u_{N_1-1,j} + u_{N_1-2,j}, \\ u_{i,0} = 3u_{i,1} - 3u_{i,2} + u_{i,3}, \quad u_{i,N_2+1} = 3u_{i,N_2} - 3u_{i,N_2-1} + u_{i,N_2-2}. \end{aligned}$$

It is trivial to incorporate Dirichlet boundary conditions (14) on $\partial\Omega'_2$ in the numerical scheme. Thus, only for illustration, we consider the case $\partial\Omega'_1 \equiv \partial\Omega'$, $\partial\Omega'_2 \equiv \emptyset$ and impose (13) on the whole boundary.

West boundary $\partial\Omega'_W$: $i = 1$, $1 < j < N_2$. From (13) we have

$$-u_{\hat{x}_{11,j}} = g'_{11,j}(\tau), \quad \text{and therefore } u_{0,j} = 2h_1 g'_{11,j}(\tau) + u_{2,j}, \quad j = 2, \dots, N_2 - 1. \quad (30)$$

Applying (29) for $i = 1$, $1 < j < N_2$, where the term $-\Lambda_1^- u_{\bar{x}_{11,j}}$ is replaced by $g'_{11,j}(\tau)$ and $u_{0,j}$, $u_{0,j\pm 1}$ are eliminated from (30), we get

$$\begin{aligned} \frac{\partial u}{\partial \tau} - \frac{\sigma_1^2}{h_1} u_{x_1} - \frac{1}{2}\sigma_2^2 u_{\bar{x}_2 x_2} - \frac{\sigma_1 \sigma_2}{2} |\rho'| (u_{x_1 x_2} - u_{x_1 \bar{x}_2}) - A_1^+ \Lambda_1^+ u_{x_1} - A_2^+ \Lambda_2^+ u_{x_2} \\ + A_2^- \Lambda_2^- u_{\bar{x}_2} + ru = A_1^- g'_1 + \frac{\sigma_1^2}{h_1} g'_1 - \sigma_1 \sigma_2 (\rho'^+ g'_{1\bar{x}_2} - \rho'^- g'_{1x_2}), \quad \rho'_{1,j} = \rho'(-g'_{1\hat{x}_{21,j}}). \end{aligned} \quad (31)$$

North boundary $\partial\Omega'_N$: $1 < i < N_1$, $j = N_2$. Now (13) is replaced by

$$u_{\hat{x}_{2i,N_2}} = g'_{1i,N_2}(\tau) \Rightarrow u_{i,N_2+1} = 2h_2 g'_{1i,N_2}(\tau) + u_{i,N_2-1}, \quad i = 2, \dots, N_1 - 1. \quad (32)$$

As before, from (29) at point (x_{1i}, x_{2N_2}, τ) , replacing $\Lambda_2^+ u_{x_{2i,N_2}}$ by $g'_{1i,N_2}(\tau)$ we obtain

$$\begin{aligned} \frac{\partial u}{\partial \tau} - \frac{1}{2}\sigma_2^2 u_{\bar{x}_1 x_1} + \frac{\sigma_2^2}{h_2} u_{\bar{x}_2} - \frac{\sigma_1 \sigma_2}{2} |\rho'| (u_{\bar{x}_1 \bar{x}_2} - u_{x_1 \bar{x}_2}) - A_1^+ \Lambda_1^+ u_{x_1} + A_1^- \Lambda_1^- u_{\bar{x}_1} \\ + A_2^- \Lambda_2^- u_{\bar{x}_2} + ru = A_2^+ g'_1 + \frac{\sigma_2^2}{h_2} g'_1 + \sigma_1 \sigma_2 (\rho'^+ g'_{1x_1} - \rho'^- g'_{1\bar{x}_1}), \quad \rho'_{i,N_2} = \rho'(g'_{1\hat{x}_{1i,N_2}}). \end{aligned} \quad (33)$$

East boundary $\partial\Omega'_E$: $i = N_1$, $1 < j < N_2$. Similarly, (13) is discretized by

$$u_{\hat{x}_{1N_1,j}} = g'_{1N_1,j}(\tau) \quad \text{and} \quad u_{N_1+1,j} = 2h_1 g'_{1N_1,j}(\tau) + u_{N_1-1,j}, \quad j = 2, \dots, N_2 - 1. \quad (34)$$

Thus, from (29) written at grid node (x_{1N_1}, x_{2j}, τ) , we get the approximation at east boundary

$$\begin{aligned} \frac{\partial u}{\partial \tau} + \frac{\sigma_1^2}{h_1} u_{\bar{x}_1} - \frac{1}{2} \sigma_2^2 u_{\bar{x}_2 x_2} - \frac{\sigma_1 \sigma_2}{2} |\rho'| (u_{\bar{x}_1 \bar{x}_2} - u_{\bar{x}_1 x_2}) + A_1^- \Lambda_1^- u_{\bar{x}_1} - A_2^+ \Lambda_2^+ u_{x_2} \\ + A_2^- \Lambda_2^- u_{\bar{x}_2} + ru = A_1^+ g'_1 + \frac{\sigma_1^2}{h_1} g'_1 + \sigma_1 \sigma_2 (\rho'^+ g'_{1x_2} - \rho'^- g'_{1\bar{x}_2}), \quad \rho'_{N_2, j} = \rho'(g'_{1\hat{x}_2 N_2, j}). \end{aligned} \quad (35)$$

South boundary $\partial\Omega'_S$: $1 < i < N_1, j = 1$. Now the corresponding discrete boundary condition in (13) is

$$u_{\hat{x}_2 i, 1} = g'_{1i, 1}(\tau) \Rightarrow u_{i, 0} = 2h_2 g'_{1i, 1}(\tau) + u_{i, 2}, \quad i = 2, \dots, N_1 - 1. \quad (36)$$

The discretization, corresponding to the south boundary is:

$$\begin{aligned} \frac{\partial u}{\partial \tau} - \frac{1}{2} \sigma_1^2 u_{\bar{x}_1 x_1} - \frac{\sigma_2^2}{h_2} u_{x_2} - \frac{\sigma_1 \sigma_2}{2} |\rho'| (u_{x_1 x_2} - u_{\bar{x}_1 x_2}) - A_1^+ \Lambda_1^+ u_{x_1} + A_1^- \Lambda_1^- u_{\bar{x}_1} \\ - A_2^+ \Lambda_2^+ u_{x_2} + ru = A_2^- g'_1 + \frac{\sigma_2^2}{h_2} g'_1 - \sigma_1 \sigma_2 (\rho'^+ g'_{1\bar{x}_1} - \rho'^- g'_{1x_1}), \quad \rho'_{i, 1} = \rho'(-g'_{1\hat{x}_1 i, 1}). \end{aligned} \quad (37)$$

North-West corner node: $i = 1, j = N_2$. Following the same technique as before, we eliminate artificial grid nodes arise in (29) (written at point $i = 1, j = N_2$), using boundary conditions (30) for $j = N_2$ and (32) for $i = 1$ and replace $A_1^- \Lambda_1^- u_{\bar{x}_1}$ by $A_1^- g'_1$ and $A_2^+ \Lambda_2^+ u_{x_2}$ by $A_2^+ g'_1$. More different is the treatment of the term u_{0, N_2+1} :

$$u_{0, N_2+1} = \begin{cases} u_{2, N_2-1} + 2h_2 g'_{12, N_2} + 2h_1 g'_{11, N_2+1}, & \text{applying first (30), then (32),} \\ u_{2, N_2-1} + 2h_2 g'_{10, N_2} + 2h_1 g'_{11, N_2-1}, & \text{applying first (32), then (30).} \end{cases}$$

Averaging the above quantities we obtain

$$\begin{aligned} u_{0, N_2+1} &= u_{2, N_2-1} + h_2 g'_{12, N_2} + h_1 g'_{11, N_2+1} + h_2 g'_{10, N_2} + h_1 g'_{11, N_2-1} \\ &= u_{1, N_2-1} + 2h_2 g'_{12, N_2} + 2h_1 g'_{11, N_2-1} + 2h_1 h_2 (g'_{1\hat{x}_2} - g'_{1\hat{x}_1})_{1, N_2}. \end{aligned}$$

To compute $\rho'(u_{\hat{x}_1 \hat{x}_2})$ at grid node $i = 1, j = N_2$ we proceed similarly:

$$u_{\hat{x}_1 \hat{x}_2} = \begin{cases} g'_{1\hat{x}_1}, & \text{applying (30),} \\ -g'_{1\hat{x}_2}, & \text{applying (32),} \end{cases} \quad u_{\hat{x}_1 \hat{x}_2} \simeq 0.5(g'_{1\hat{x}_1} - g'_{1\hat{x}_2}) \Rightarrow \rho'(u_{\hat{x}_1 \hat{x}_2}) \simeq \rho'(g'_{1\hat{x}_1} - g'_{1\hat{x}_2}),$$

as we need only the sign of $u_{\hat{x}_1 \hat{x}_2}$.

Consequently, the approximation at North-West corner node is

$$\begin{aligned} \frac{\partial u}{\partial \tau} - \frac{\sigma_1^2}{h_1} u_{x_1} + \frac{\sigma_2^2}{h_2} u_{\bar{x}_2} + \sigma_1 \sigma_2 |\rho'| u_{x_1 \bar{x}_2} - A_1^+ \Lambda_1^+ u_{x_1} + A_2^- \Lambda_2^- u_{\bar{x}_2} + ru \\ = (A_1^- + A_2^+) g'_1 + \left(\frac{\sigma_1^2}{h_1} + \frac{\sigma_2^2}{h_2} \right) g'_1 + \sigma_1 \sigma_2 \rho'^+ (g'_{1x_1} - g'_{1\bar{x}_2}) + \sigma_1 \sigma_2 \rho'^- G_{NW}, \quad \text{where} \quad (38) \\ G_{NW} = g'_{1x_1} - g'_{1\bar{x}_2} + g'_{1\hat{x}_2} - g'_{1\hat{x}_1} \quad \text{and} \quad \rho'_{1, N_2} = \rho'[(g'_{1\hat{x}_1} - g'_{1\hat{x}_2})_{1, N_2}]. \end{aligned}$$

North-East corner node: $i = N_1, j = N_2$. From (29), (32) and (34) at point $i = N_1, j = N_2$ we get

$$\begin{aligned} & \frac{\partial u}{\partial \tau} + \frac{\sigma_1^2}{h_1} u_{\bar{x}_1} + \frac{\sigma_2^2}{h_2} u_{\bar{x}_2} - \sigma_1 \sigma_2 |\rho'| u_{\bar{x}_1 \bar{x}_2} + A_1^- \Lambda_1^- u_{\bar{x}_1} + A_2^- \Lambda_2^- u_{\bar{x}_2} + ru \\ &= (A_1^+ + A_2^+) g'_1 + \left(\frac{\sigma_1^2}{h_1} + \frac{\sigma_2^2}{h_2} \right) g'_1 - \sigma_1 \sigma_2 \rho'^+ G_{NE} - \sigma_1 \sigma_2 \rho'^- (g'_{1\bar{x}_1} + g'_{1\bar{x}_2}), \quad \text{where} \quad (39) \\ & G_{NE} = g'_{1\bar{x}_1} + g'_{1\bar{x}_2} - g'_{1\hat{x}_2} - g'_{1\hat{x}_1} \quad \text{and} \quad \rho'_{1,N_2} = \rho'[(g'_{1\hat{x}_1} + g'_{1\hat{x}_2})_{1,N_2}]. \end{aligned}$$

South-East corner node: $i = N_1, j = 1$. Again, from (29), (34) and (36) at point $i = N_1, j = 1$ we have

$$\begin{aligned} & \frac{\partial u}{\partial \tau} + \frac{\sigma_1^2}{h_1} u_{\bar{x}_1} - \frac{\sigma_2^2}{h_2} u_{x_2} + \sigma_1 \sigma_2 |\rho'| u_{\bar{x}_1 x_2} + A_1^- \Lambda_1^- u_{\bar{x}_1} - A_2^+ \Lambda_2^+ u_{x_2} + ru \\ &= (A_1^+ + A_2^-) g'_1 + \left(\frac{\sigma_1^2}{h_1} + \frac{\sigma_2^2}{h_2} \right) g'_1 - \sigma_1 \sigma_2 \rho'^+ (g'_{1\bar{x}_1} - g'_{1x_2}) - \sigma_1 \sigma_2 \rho'^- G_{SE}, \quad \text{where} \quad (40) \\ & G_{SE} = g'_{1\bar{x}_1} - g'_{1x_2} - g'_{1\hat{x}_1} + g'_{1\hat{x}_2} \quad \text{and} \quad \rho'_{N_1,1} = \rho'[(g'_{1\hat{x}_2} - g'_{1\hat{x}_1})_{N_1,1}]. \end{aligned}$$

South-West corner node: $i = j = 1$. As before, from (29), (30) and (36) at point $i = 1, j = 1$ we obtain

$$\begin{aligned} & \frac{\partial u}{\partial \tau} - \frac{\sigma_1^2}{h_1} u_{x_1} - \frac{\sigma_2^2}{h_2} u_{x_2} - \sigma_1 \sigma_2 |\rho'| u_{x_1 x_2} - A_1^+ \Lambda_1^+ u_{x_1} - A_2^+ \Lambda_2^+ u_{x_2} + ru \\ &= (A_1^- + A_2^-) g'_1 + \left(\frac{\sigma_1^2}{h_1} + \frac{\sigma_2^2}{h_2} \right) g'_1 + \sigma_1 \sigma_2 \rho'^+ (g'_{1x_1} + g'_{1x_2}) + \sigma_1 \sigma_2 \rho'^- G_{SW}, \quad \text{where} \quad (41) \\ & G_{SW} = g'_{1x_1} + g'_{1x_2} - g'_{1\hat{x}_1} - g'_{1\hat{x}_2} \quad \text{and} \quad \rho'_{1,1} = \rho'[(-g'_{1\hat{x}_1} - g'_{1\hat{x}_2})_{1,1}]. \end{aligned}$$

Now, we are going to investigate conditions, which guarantee the positivity preserving property of the semi-discrete problem. Further we need the following well known results.

Consider the initial value problem (IVP) for the ODE system

$$u'(\tau) = g(\tau, u(\tau)), \quad \tau \geq \tau_0, \quad u(\tau_0) = u^0, \quad \tau_0 \in \mathbb{R}, \quad u^0 \in \mathbb{R}^p, \quad g : \mathbb{R} \times \mathbb{R}^p \rightarrow \mathbb{R}^p \quad (42)$$

Definition 1 ([6], **Positive ODE system, positive semi-discretization**) *The ODE in (42) and the IVP (42) are said to be positive if g is continuous and (42) has a unique solution for all τ_0 and for all u^0 , and $u(\tau) \geq 0$ holds for all $\tau \geq \tau_0$ whenever $u^0 \geq 0$. A semi-discretization of a given PDE (with non-negative solution) is called positive if it leads to a positive ODE system.*

Lemma 2 ([7]) *Let g be continuous and (42) has a unique solution for all τ_0 and for all u_0 . The initial value problem (42) is positive if and only if*

$$v_i = 0, \quad v_j \geq 0 \quad \text{for all } j \neq i \quad \Rightarrow \quad g_i(\tau, v) \geq 0,$$

holds for all τ and any vector $v \in \mathbb{R}^p$ and all $i = 1, \dots, p$.

As a consequence of Lemma 2 is

Corollary 1 ([9, p. 34]) *A linear system $u'(\tau) = Au(\tau)$, $A = \{a_{i,j}\}$ is positive iff $a_{i,j} \geq 0$ for all $i \neq j$.*

Guided by this results, we can apply (just as in [6]) the statement of Lemma 2 and Corollary 1 for the numerical discretization of of (10)-(14), written in the form

$$\begin{aligned} \frac{du}{d\tau} = & C_{i+1,j}u_{i+1,j} + C_{i-1,j}u_{i-1,j} + C_{i,j+1}u_{i,j+1} + C_{i,j-1}u_{i,j-1} + C_{i+1,j-1}u_{i+1,j-1} \\ & + C_{i-1,j-1}u_{i-1,j-1} + C_{i-1,j+1}u_{i-1,j+1} + C_{i+1,j+1}u_{i+1,j+1} \\ & - C_{i,j}u_{i,j} + g(\tau), \quad i = 1, \dots, N_1, \quad j = 1, \dots, N_2. \end{aligned} \quad (43)$$

Lemma 3 *The ODE system, defined by (43) is positive, if all coefficients $C_{\Sigma_{i,j}} = \{C_{i\pm 1,j}, C_{i,j\pm 1}, C_{i\pm 1,j\pm 1}\}$ are non-negative and $g(\tau) \geq 0$.*

Proof. The results follows from Lemma 2. □

Theorem 4 *The numerical discretization (29), combined with Dirichlet boundary conditions (on $\partial\Omega'_2$) and approximations (31), (33), (35), (37) and (38), (39), (40), (41) of the Neumann boundary conditions, depending on the boundary $\partial\Omega'_1$, is positive, if*

$$\begin{aligned} \frac{\sigma_1}{\sigma_2} \max_{\substack{1+b_W \leq i \leq N_1-b_E \\ 1+b_S \leq j \leq N_2-b_N}} |\rho'| \leq \frac{h_1}{h_2} \leq \frac{\sigma_1}{\sigma_2 \max_{\substack{1+b_W \leq i \leq N_1-b_E \\ 1+b_S \leq j \leq N_2-b_N}} |\rho'|}, \quad \text{where} \\ b_Q = \begin{cases} 1, & \partial\Omega'_Q \subseteq \partial\Omega'_2, \\ 0, & \text{elsewhere} \end{cases}, \quad Q = \{W, E, N, S\}. \end{aligned} \quad (44)$$

Proof. First we consider the discretization (29) at inner points: $2 < i < N_1 - 1$, $2 < j < N_2 - 1$. Taking into account that $|\rho'_{i,j}| = \rho'^+_{i,j} + \rho'^-_{i,j}$, the coefficients, corresponding to (43) are

$$\begin{aligned} C_{i\pm 1,j} &= \frac{\sigma_1^2}{2h_1^2} - \frac{\sigma_1\sigma_2|\rho'_{i,j}|}{2h_1h_2} + \frac{A_1^\pm \Lambda_{1,i,j}^\pm}{h_1}, \\ C_{i,j\pm 1} &= \frac{\sigma_2^2}{2h_2^2} - \frac{\sigma_1\sigma_2|\rho'_{i,j}|}{2h_1h_2} + \frac{A_2^\pm \Lambda_{2,i,j}^\pm}{h_2}, \\ C_{i-1,j+1} = C_{i+1,j-1} &= \frac{\sigma_1\sigma_2\rho'^-}{2h_1h_2}, \quad C_{i-1,j-1} = C_{i+1,j+1} = \frac{\sigma_1\sigma_2\rho'^+}{2h_1h_2}, \quad g \equiv 0. \end{aligned}$$

To ensure the condition of Lemma 3 we require

$$\frac{\sigma_1}{\sigma_2} \max_{\substack{1 < i < N_1 \\ 1 < j < N_2}} |\rho'| \leq \frac{h_1}{h_2} \leq \frac{\sigma_1}{\sigma_2 \max_{\substack{1 < i < N_1 \\ 1 < j < N_2}} |\rho'|}. \quad (45)$$

For equation, corresponding to Neumann condition imposed on the East boundary ($i = N_1$, $1 < j < N_2$) from (35) we have

$$\begin{aligned} C_{N_1-1,j} &= \frac{\sigma_1^2}{h_1^2} - \frac{\sigma_1\sigma_2|\rho'_{N_1,j}|}{h_1h_2} + \frac{A_1^- \Lambda_{1,N_1,j}^-}{h_1}, \\ C_{N_1,j\pm 1} &= \frac{\sigma_2^2}{2h_2^2} - \frac{\sigma_1\sigma_2|\rho'_{N_1,j}|}{2h_1h_2} + \frac{A_2^\pm \Lambda_{2,N_1,j}^\pm}{h_2}, \\ C_{N_1-1,j\pm 1} &= \frac{\sigma_1\sigma_2|\rho'_{N_1,j}|}{2h_1h_2}, \quad g_{N_1,j} = A_1^+ g'_{N_1,j} + \frac{\sigma_1^2}{h_1} g'_{N_1,j} + \sigma_1\sigma_2(\rho'^+ g'_{1x_2} - \rho'^- g'_{1\bar{x}_2})_{N_1,j}. \end{aligned}$$

It is easy to verify that $C_{\Sigma_{N_1,j}} \geq 0$ and $g_{i,N_2} \geq 0$ if

$$\frac{\sigma_1}{\sigma_2} \max_{1 < j < N_2} |\rho'_{N_1,j}| \leq \frac{h_1}{h_2} \leq \frac{\sigma_1}{\sigma_2 \max_{1 < j < N_2} |\rho'_{N_1,j}|}. \quad (46)$$

Similarly, from (31), (33), (37), corresponding to Neumann boundary condition on $\partial\Omega'_{\{W,S,N\}}$ respectively, to guarantee that $C_{\Sigma_{\partial\Omega'_{\{W,S,N\}}}} \geq 0$ and $g_{\partial\Omega'_{\{W,S,N\}}} \geq 0$, we obtain the estimates

$$\begin{aligned} \frac{\sigma_1}{\sigma_2} \max_{1 < j < N_2} |\rho'_{1,j}| &\leq \frac{h_1}{h_2} \leq \frac{\sigma_1}{\sigma_2 \max_{1 < j < N_2} |\rho'_{1,j}|}, \\ \frac{\sigma_1}{\sigma_2} \max_{1 < i < N_1} |\rho'_{i,1}| &\leq \frac{h_1}{h_2} \leq \frac{\sigma_1}{\sigma_2 \max_{1 < i < N_1} |\rho'_{i,1}|}, \quad \frac{\sigma_1}{\sigma_2} \max_{1 < i < N_1} |\rho'_{i,N_2}| \leq \frac{h_1}{h_2} \leq \frac{\sigma_1}{\sigma_2 \max_{1 < i < N_1} |\rho'_{i,N_2}|} \end{aligned} \quad (47)$$

Similar estimate is obtained from the discretizations at the corner node, where the two Neumann boundaries intersect. For example, let $\{\partial\Omega'_N, \partial\Omega'_E\} \subseteq \partial\Omega'_1$, then from (39) for all elements of $C_{\Sigma_{N_1,N_2}}$ and g_{N_1,N_2} we have

$$\begin{aligned} C_{N_1-1,N_2} &= \frac{\sigma_1^2}{h_1^2} - \frac{\sigma_1\sigma_2|\rho'_{N_1,N_2}|}{h_1h_2} + \frac{A_1^- \Lambda_{1,N_1,N_2}^-}{h_1}, \\ C_{N_1,N_2-1} &= \frac{\sigma_2^2}{h_2^2} - \frac{\sigma_1\sigma_2|\rho'_{N_1,N_2}|}{h_1h_2} + \frac{A_2^- \Lambda_{2,N_1,N_2}^-}{h_2}, \quad C_{N_1-1,N_2-1} = \frac{\sigma_1\sigma_2|\rho'_{N_1,N_2}|}{h_1h_2}, \\ g_{N_1,N_2} &= \left(A_1^+ + A_2^+ + \frac{\sigma_1^2}{h_1} + \frac{\sigma_2^2}{h_2} \right) g'_{N_1,N_2} - \sigma_1\sigma_2[\rho'^+ G_{NE} + \rho'^- (g'_{1\bar{x}_1} + g'_{1\bar{x}_2})]_{N_1,N_2}. \end{aligned}$$

The requirement $C_{\Sigma_{N_1,N_2}} \geq 0$ and $g_{N_1,N_2} \geq 0$ leads to the estimate

$$\frac{\sigma_1}{\sigma_2} |\rho'_{N_1,N_2}| \leq \frac{h_1}{h_2} \leq \frac{\sigma_1}{\sigma_2 |\rho'_{N_1,N_2}|}. \quad (48)$$

Similarly, from (38), (40), (41) we get

$$\frac{\sigma_1}{\sigma_2} |\rho'_{1,N_2}| \leq \frac{h_1}{h_2} \leq \frac{\sigma_1}{\sigma_2 |\rho'_{1,N_2}|}, \quad \frac{\sigma_1}{\sigma_2} |\rho'_{N_1,1}| \leq \frac{h_1}{h_2} \leq \frac{\sigma_1}{\sigma_2 |\rho'_{N_1,1}|}, \quad \frac{\sigma_1}{\sigma_2} |\rho'_{1,1}| \leq \frac{h_1}{h_2} \leq \frac{\sigma_1}{\sigma_2 |\rho'_{1,1}|}. \quad (49)$$

Collecting all results (45)-(49), we obtain (44). \square

4 Full discretization

In this section we develop an implicit-explicit second-order numerical algorithm which preserves the positivity property of the solution. A semi-implicit and implicit method are used for the diffusion (the non-linear term is computed at the old time level) and reaction terms respectively while the convection term is approximated explicitly.

The grid points over the time interval $[0, T]$ are defined by $\tau_n = \tau_{n-1} + \Delta\tau$, $n = 1, 2, \dots$, $\tau_0 = 0$. Approximations of $u(x_i, y_j, \tau_n)$ is denoted by $u_{i,j}^n$, but further for simplicity, we use the notations $\hat{u}_{i,j} := u_{i,j}^n$ and $u_{i,j} := u_{i,j}^{n-1}$, $\hat{u}_t := (\hat{u} - u)/\Delta\tau$

The full discretization of (29) is

$$\begin{aligned} \hat{u}_t - \frac{1}{2}\sigma_1^2\hat{u}_{\bar{x}_1x_1} - \frac{1}{2}\sigma_2^2\hat{u}_{\bar{x}_2x_2} - \sigma_1\sigma_2(\rho'^+\hat{u}_{x_1x_2}^+ - \rho'^-\hat{u}_{x_1x_2}^-) + r\hat{u} = A_1^+\Lambda_1^+u_{x_1} - A_1^-\Lambda_1^-u_{\bar{x}_1} \\ + A_2^+\Lambda_2^+u_{x_2} - A_2^-\Lambda_2^-u_{\bar{x}_2}, \quad i = 2, \dots, N_1 - 1, \quad j = 2, \dots, N_2 - 1. \end{aligned} \quad (50)$$

For non-homogeneous Neumann boundaries (13) (if any) we obtain from (31), (33), (35),(37), the following discretization

$$\begin{aligned} \hat{u}_t - \frac{\sigma_1^2}{h_1}\hat{u}_{x_1} - \frac{1}{2}\sigma_2^2\hat{u}_{\bar{x}_2x_2} - \frac{\sigma_1\sigma_2}{2}|\rho'|(\hat{u}_{x_1x_2} - \hat{u}_{x_1\bar{x}_2}) + r\hat{u} = A_1^+\Lambda_1^+u_{x_1} + A_2^+\Lambda_2^+u_{x_2} \\ - A_2^-\Lambda_2^-u_{\bar{x}_2} + A_1^-\hat{g}'_1 + \frac{\sigma_1^2}{h_1}\hat{g}'_1 - \sigma_1\sigma_2(\rho'^+\hat{g}'_{1\bar{x}_2} - \rho'^-\hat{g}'_{1x_2}), \quad i = 1, \quad j = 2, \dots, N_2 - 1. \end{aligned} \quad (51)$$

$$\begin{aligned} \hat{u}_t - \frac{1}{2}\sigma_2^2\hat{u}_{\bar{x}_1x_1} + \frac{\sigma_2^2}{h_2}\hat{u}_{\bar{x}_2} - \frac{\sigma_1\sigma_2}{2}|\rho'|(\hat{u}_{\bar{x}_1\bar{x}_2} - \hat{u}_{x_1\bar{x}_2}) + r\hat{u} = A_1^+\Lambda_1^+u_{x_1} - A_1^-\Lambda_1^-u_{\bar{x}_1} \\ - A_2^-\Lambda_2^-u_{\bar{x}_2} + A_2^+\hat{g}'_1 + \frac{\sigma_2^2}{h_2}\hat{g}'_1 + \sigma_1\sigma_2(\rho'^+\hat{g}'_{1x_1} - \rho'^-\hat{g}'_{1\bar{x}_1}), \quad i = 2, \dots, N_1 - 1, \quad j = N_2. \end{aligned} \quad (52)$$

$$\begin{aligned} \hat{u}_t + \frac{\sigma_1^2}{h_1}\hat{u}_{\bar{x}_1} - \frac{1}{2}\sigma_2^2\hat{u}_{\bar{x}_2x_2} - \frac{\sigma_1\sigma_2}{2}|\rho'|(\hat{u}_{\bar{x}_1\bar{x}_2} - \hat{u}_{\bar{x}_1x_2}) + r\hat{u} = -A_1^-\Lambda_1^-u_{\bar{x}_1} + A_2^+\Lambda_2^+u_{x_2} \\ - A_2^-\Lambda_2^-u_{\bar{x}_2} + A_1^+\hat{g}'_1 + \frac{\sigma_1^2}{h_1}\hat{g}'_1 + \sigma_1\sigma_2(\rho'^+\hat{g}'_{1x_2} - \rho'^-\hat{g}'_{1\bar{x}_2}), \quad i = N_1, \quad j = 2, \dots, N_2 - 1. \end{aligned} \quad (53)$$

$$\begin{aligned} \hat{u}_t - \frac{1}{2}\sigma_1^2\hat{u}_{\bar{x}_1x_1} - \frac{\sigma_2^2}{h_2}\hat{u}_{x_2} - \frac{\sigma_1\sigma_2}{2}|\rho'|(\hat{u}_{x_1x_2} - \hat{u}_{\bar{x}_1x_2}) + r\hat{u} = A_1^+\Lambda_1^+u_{x_1} - A_1^-\Lambda_1^-u_{\bar{x}_1} \\ + A_2^+\Lambda_2^+u_{x_2} + A_2^-\hat{g}'_1 + \frac{\sigma_2^2}{h_2}\hat{g}'_1 - \sigma_1\sigma_2(\rho'^+\hat{g}'_{1\bar{x}_1} - \rho'^-\hat{g}'_{1x_1}), \quad i = 2, \dots, N_1 - 1, \quad j = 1. \end{aligned} \quad (54)$$

Finally, for the corner nodes, where the two Neumann boundaries intersects, from (38), (39), (40), (41) we have

$$\begin{aligned} \hat{u}_t - \frac{\sigma_1^2}{h_1}\hat{u}_{x_1} + \frac{\sigma_2^2}{h_2}\hat{u}_{\bar{x}_2} + \sigma_1\sigma_2|\rho'|\hat{u}_{x_1\bar{x}_2} + r\hat{u} = A_1^+\Lambda_1^+u_{x_1} - A_2^-\Lambda_2^-u_{\bar{x}_2} + (A_1^- + A_2^+)\hat{g}'_1 \\ + \left(\frac{\sigma_1^2}{h_1} + \frac{\sigma_2^2}{h_2}\right)\hat{g}'_1 + \sigma_1\sigma_2\rho'^+(\hat{g}'_{1x_1} - \hat{g}'_{1\bar{x}_2}) + \sigma_1\sigma_2\rho'^-\hat{G}_{NW}, \quad i = 1, \quad j = N_2. \end{aligned} \quad (55)$$

$$\begin{aligned} \hat{u}_t + \frac{\sigma_1^2}{h_1}\hat{u}_{\bar{x}_1} + \frac{\sigma_2^2}{h_2}\hat{u}_{\bar{x}_2} - \sigma_1\sigma_2|\rho'|\hat{u}_{\bar{x}_1\bar{x}_2} + r\hat{u} = -A_1^-\Lambda_1^-u_{\bar{x}_1} - A_2^-\Lambda_2^-u_{\bar{x}_2} + (A_1^+ + A_2^+)\hat{g}'_1 \\ + \left(\frac{\sigma_1^2}{h_1} + \frac{\sigma_2^2}{h_2}\right)\hat{g}'_1 - \sigma_1\sigma_2\rho'^+\hat{G}_{NE} - \sigma_1\sigma_2\rho'^-(\hat{g}'_{1\bar{x}_1} + \hat{g}'_{1x_2}), \quad i = N_1, \quad j = N_2. \end{aligned} \quad (56)$$

$$\begin{aligned} \hat{u}_t + \frac{\sigma_1^2}{h_1}\hat{u}_{\bar{x}_1} - \frac{\sigma_2^2}{h_2}\hat{u}_{x_2} + \sigma_1\sigma_2|\rho'|\hat{u}_{\bar{x}_1x_2} + r\hat{u} = -A_1^-\Lambda_1^-u_{\bar{x}_1} + A_2^+\Lambda_2^+u_{x_2} + (A_1^+ + A_2^-)\hat{g}'_1 \\ + \left(\frac{\sigma_1^2}{h_1} + \frac{\sigma_2^2}{h_2}\right)\hat{g}'_1 - \sigma_1\sigma_2\rho'^+(\hat{g}'_{1\bar{x}_1} - \hat{g}'_{1x_2}) - \sigma_1\sigma_2\rho'^-\hat{G}_{SE}, \quad i = N_1, \quad j = 1. \end{aligned} \quad (57)$$

$$\begin{aligned}
\widehat{u}_t - \frac{\sigma_1^2}{h_1} \widehat{u}_{x_1} - \frac{\sigma_2^2}{h_2} \widehat{u}_{x_2} - \sigma_1 \sigma_2 |\rho'| \widehat{u}_{x_1 x_2} + r \widehat{u} &= A_1^+ \Lambda_1^+ u_{x_1} + A_2^+ \Lambda_2^+ u_{x_2} + (A_1^- + A_2^-) \widehat{g}'_1 \\
&+ \left(\frac{\sigma_1^2}{h_1} + \frac{\sigma_2^2}{h_2} \right) \widehat{g}'_1 + \sigma_1 \sigma_2 \rho'^+ (\widehat{g}'_{1x_1} + \widehat{g}'_{1x_2}) + \sigma_1 \sigma_2 \rho'^- \widehat{G}_{SW}, \quad i = 1, \quad j = 1.
\end{aligned} \tag{58}$$

Next, we discuss positivity preserving property and stability of the numerical solution.

The system (50), associated with Dirichlet boundary conditions and the discretization (51)-(58), in the case of Neumann boundary can be written in the following compact form

$$\begin{aligned}
&-C_{i+1,j} \widehat{u}_{i+1,j} - C_{i-1,j} \widehat{u}_{i-1,j} - C_{i,j+1} \widehat{u}_{i,j+1} - C_{i,j-1} \widehat{u}_{i,j-1} - C_{i+1,j-1} \widehat{u}_{i+1,j-1} \\
&-C_{i-1,j-1} \widehat{u}_{i-1,j-1} - C_{i-1,j+1} \widehat{u}_{i-1,j+1} - C_{i+1,j+1} \widehat{u}_{i+1,j+1} + C_{i,j} \widehat{u}_{i,j} = f_{i,j},
\end{aligned} \tag{59}$$

for $i = 1, \dots, N_1$, $j = 1, \dots, N_2$ and equivalent matrix form

$$\begin{aligned}
&\mathcal{M} \widehat{U} = \mathcal{F}, \quad \text{where} \\
U &= \underbrace{[u_{1,1}, u_{2,1}, \dots, u_{N_1,1}, \dots]}_{j=1}, \underbrace{[u_{1,j}, u_{2,j}, \dots, u_{N_1,j}, \dots]}_{2 \leq j \leq N_2-1}, \underbrace{[u_{1,N_2}, u_{2,N_2}, \dots, u_{N_1,N_2}]}_{j=N_2}^T,
\end{aligned}$$

where $\mathcal{M} = \{m_{k,p}\}$ is a square $N_1 N_2 \times N_1 N_2$ matrix and $\mathcal{F} = \{f_k\}$, $k = i + (j - 1)N_1$ is a column-vectors with $N_1 N_2$ known from the previous time level entries.

Following Corollary 3.20 [26, p.91], if \mathcal{M} is diagonal dominant matrix with $m_{k,p} \leq 0$ for all $k \neq p$ and $m_{k,k} > 0$ for all $1 \leq k \leq N_1 N_2$, then $\mathcal{M}^{-1} > 0$. Thus, if $\mathcal{F} \geq 0$, we can conclude that $\widehat{U} \geq 0$. On this base we can prove the following statement

Theorem 5 *If $g_s \geq 0$, $s = 0, 1, 2$, (44) holds and*

$$\Delta \tau \leq \frac{h_1 h_2}{2(|A_1| h_2 + |A_2| h_1)}, \tag{60}$$

then the numerical solution of the problem (10)-(14) (respectively (4)-(8)), obtained by (50), associated with Dirichlet boundary conditions and discretization (51)-(58) (depending on $\partial\Omega$) is non-negative.

Proof. We apply induction method: the statement holds for $\tau_0 = 0$, assume that it holds at time τ_{n-1} and prove that this statement holds at time τ_n . Thus, via to the time integration, the corresponding assertion holds at each time level. Let $u^{n-1} \geq 0$.

First, using the compact form (59) of the presented numerical scheme, we show that $\mathcal{M}^{-1} > 0$, which means that matrix \mathcal{M} posses the above mentioned property, i.e. for all $i = 1, \dots, N_1$ and $j = 1, \dots, N_2$:

P1. \mathcal{M} is diagonally dominant, which is equivalent to $|C_{i,j}| \geq \sum_{C_{i+s_1, j+s_2} \in C_{\Sigma_{i,j}}} |C_{i+s_1, j+s_2}|$;

P2. $m_{k,p} \leq 0$ for all $k \neq p$, equivalently to $C_{i+s_1, j+s_2} \geq 0$ for all $C_{i+s_1, j+s_2} \in C_{\Sigma_{i,j}}$;

P3. $m_{k,k} > 0$ for all $1 \leq k \leq N_1 N_2$, equivalently to $C_{i,j} > 0$.

Then we find the condition which guarantees

P4. the non-negativity of the right-hand side \mathcal{F} .

At inner points $2 \leq i \leq N_1 - 1$, $2 \leq j \leq N_2 - 1$ from (50) we get the corresponding coefficients of (59) and \mathcal{F}

$$\begin{aligned}
C_{i,j} &= \frac{1}{\Delta\tau} + \frac{\sigma_1^2}{h_1^2} + \frac{\sigma_2^2}{h_2^2} - \frac{\sigma_1\sigma_2|\rho'_{i,j}|}{h_1h_2} + r, \quad C_{i\pm 1,j} = \frac{\sigma_1^2}{2h_1^2} - \frac{\sigma_1\sigma_2|\rho'_{i,j}|}{2h_1h_2}, \quad C_{i,j\pm 1} = \frac{\sigma_2^2}{2h_2^2} - \frac{\sigma_1\sigma_2|\rho'_{i,j}|}{2h_1h_2}, \\
C_{i-1,j+1} &= C_{i+1,j-1} = \frac{\sigma_1\sigma_2\rho'_{i,j}^-}{2h_1h_2}, \quad C_{i-1,j-1} = C_{i+1,j+1} = \frac{\sigma_1\sigma_2\rho'_{i,j}^+}{2h_1h_2}, \\
f_{i,j} &= \frac{1}{\Delta\tau}u_{i,j} + A_1^+\Lambda_{1,i,j}^+ \frac{u_{i+1,j} - u_{i,j}}{h_1} - A_1^-\Lambda_{1,i,j}^- \frac{u_{i,j} - u_{i-1,j}}{h_1} \\
&\quad + A_2^+\Lambda_{2,i,j}^+ \frac{u_{i,j+1} - u_{i,j}}{h_2} - A_2^-\Lambda_{2,i,j}^- \frac{u_{i,j} - u_{i,j-1}}{h_2},
\end{aligned} \tag{61}$$

Properties P1 - P3 are fulfilled, owing to (44). We have $|C_{i,j}| - \sum_{C_{i+s_1,j+s_2} \in C_{\Sigma_{i,j}}} |C_{i+s_1,j+s_2}| = \frac{1}{\tau} + r$, $C_{i,j} \geq \frac{1}{\tau} + r > 0$ and all $C_{i+s_1,j+s_2} \in C_{\Sigma_{i,j}}$ are non-negative. To ensure the property P4 we require

$$\frac{1}{\Delta\tau} - \frac{A_1^+\Lambda_{1,i,j}^+}{h_1} - \frac{A_1^-\Lambda_{1,i,j}^-}{h_1} - \frac{A_2^+\Lambda_{2,i,j}^+}{h_2} - \frac{A_2^-\Lambda_{2,i,j}^-}{h_2} \geq 0,$$

which leads to restriction (60).

Let for instance $\partial\Omega'_E \subseteq \partial\Omega'_1$. Thus from (53) we have

$$\begin{aligned}
C_{N_1,j} &= \frac{1}{\Delta\tau} + \frac{\sigma_1^2}{h_1^2} + \frac{\sigma_2^2}{h_2^2} - \frac{\sigma_1\sigma_2|\rho'_{N_1,j}|}{h_1h_2} + r, \quad C_{N_1-1,j} = \frac{\sigma_1^2}{h_1^2} - \frac{\sigma_1\sigma_2|\rho'_{N_1,j}|}{h_1h_2}, \\
C_{N_1,j\pm 1} &= \frac{\sigma_2^2}{2h_2^2} - \frac{\sigma_1\sigma_2|\rho'_{N_1,j}|}{2h_1h_2}, \quad C_{N_1-1,j\pm 1} = \frac{\sigma_1\sigma_2|\rho'_{N_1,j}|}{2h_1h_2}, \\
f_{N_1,j} &= \frac{1}{\Delta\tau}u_{N_1,j} + \left(A_1^+ + \frac{\sigma_1^2}{h_1} - \frac{\sigma_1\sigma_2|\rho'_{N_1,j}|}{h_2} \right) \tilde{g}'_{1N_1,j} + \frac{\sigma_1\sigma_2\rho'_{N_1,j}^+}{h_2} \tilde{g}'_{1N_1,j+1} + \frac{\sigma_1\sigma_2\rho'_{N_1,j}^-}{h_2} \tilde{g}'_{1N_1,j-1} \\
&\quad - A_1^-\Lambda_{1N_1,j}^- \frac{u_{N_1,j} - u_{N_1-1,j}}{h_1} + A_2^+\Lambda_{2N_1,j}^+ \frac{u_{N_1,j+1} - u_{N_1,j}}{h_2} - A_2^-\Lambda_{2N_1,j}^- \frac{u_{N_1,j} - u_{N_1,j-1}}{h_2},
\end{aligned} \tag{62}$$

As before P1 - P3 follows from (44). The right-hand side is non-negative if additionally to (44) we have

$$\frac{1}{\Delta\tau} - \frac{A_1^-\Lambda_{1N_1,j}^-}{h_1} - \frac{A_2^+\Lambda_{2N_1,j}^+}{h_2} - \frac{A_2^-\Lambda_{2N_1,j}^-}{h_2} \geq 0 \quad \text{and therefore restriction (60).}$$

From equations (51), (52) and (54) we obtain similar results.

Consider now the corner node $i = N_1$, $j = N_2$, $\{\partial\Omega'_N, \partial\Omega'_E\} \subseteq \partial\Omega'_1$. From (56) we determine

$$\begin{aligned}
C_{N_1,N_2} &= \frac{1}{\Delta\tau} + \frac{\sigma_1^2}{h_1^2} + \frac{\sigma_2^2}{h_2^2} - \frac{\sigma_1\sigma_2|\rho'_{N_1,N_2}|}{h_1h_2} + r, \quad C_{N_1-1,N_2} = \frac{\sigma_1^2}{h_1^2} - \frac{\sigma_1\sigma_2|\rho'_{N_1,N_2}|}{h_1h_2}, \\
C_{N_1,N_2-1} &= \frac{\sigma_2^2}{h_2^2} - \frac{\sigma_1\sigma_2|\rho'_{N_1,N_2}|}{h_1h_2}, \quad C_{N_1-1,N_2-1} = \frac{\sigma_1\sigma_2|\rho'_{N_1,N_2}|}{h_1h_2},
\end{aligned}$$

$$\begin{aligned}
f_{N_1, N_2} = & \frac{1}{\Delta\tau} u_{N_1, N_2} + \left(A_1^+ + A_2^+ + \frac{\sigma_1^2}{h_1} + \frac{\sigma_2^2}{h_2} - \frac{\sigma_1\sigma_2|\rho'_{N_1, j}|}{h_2} - \frac{\sigma_1\sigma_2|\rho'_{N_1, j}|}{h_1} \right) \widehat{g}'_{1_{N_1, N_2}} \\
& + \frac{\sigma_1\sigma_2}{2h_2} \left[\left(|\rho'_{N_1, N_2}| + \rho'_{N_1, j} \right) \widehat{g}'_{1_{N_1, N_2-1}} + \rho'_{N_1, N_2} \widehat{g}'_{1_{N_1, N_2+1}} \right] \\
& + \frac{\sigma_1\sigma_2}{2h_1} \left[\left(|\rho'_{N_1, N_2}| + \rho'_{N_1, j} \right) \widehat{g}'_{1_{N_1-1, N_2}} + \rho'_{N_1, N_2} \widehat{g}'_{1_{N_1+1, N_2}} \right] \\
& - A_1^- \Lambda_{1_{N_1, N_2}}^- \frac{u_{N_1, N_2} - u_{N_1-1, N_2}}{h_1} - A_2^- \Lambda_{2_{N_1, N_2}}^- \frac{u_{N_1, N_2} - u_{N_1, N_2-1}}{h_2},
\end{aligned} \tag{63}$$

Evidently, restrictions (44) and (60) guarantees properties P1 - P4. Similar considerations can be applied for (55), (57) and (58). \square

The next results concern the stability of the presented numerical method.

Theorem 6 *If $\partial\Omega_1 \equiv \emptyset$ or $\partial\Omega_1 \neq \emptyset$ and $g_1 = 0$, $g_s \geq 0$, $s = 0, 2$ both (44) and (60) hold, then the numerical solution of the problem (10)-(14) (respectively (4)-(8)), obtained by (50), associated with Dirichlet boundary conditions and discretization (51)-(58) (depending on $\partial\Omega$) is stable (in maximal discrete norm) with respect to the initial and boundary conditions.*

Proof. Without loss of generality we will consider (61), (62) and (63). The estimates for the other part of the boundary are similar. Let $\|u\| := \max_{i,j} |u_{i,j}|$. Taking into account restrictions (44) and (60), from (59) and (61) we estimate

$$\|\widehat{u}\| \leq \frac{1}{1+r\Delta\tau} \|u\|. \tag{64}$$

Similarly, from (59), (62) and (63) we again obtain (64).

For homogeneous Neumann boundary conditions we apply the same considerations and after time integration procedure we set

$$\|u\| \leq \max\{\|g'_0\|, T \max_{\partial\Omega'_2} g'_2\}. \tag{65}$$

Theorem 7 *If $g_s \geq 0$, $s = 0, 1, 2$, $g_1 \neq 0$, $\partial\Omega_1 \neq \emptyset$, (44), (60) hold then the numerical solution of the problem (10)-(14) (respectively (4)-(8)), obtained by (50), associated with Dirichlet boundary conditions and discretization (51)-(58) (depending on $\partial\Omega$) is stable (in maximal discrete norm) with respect to the initial and boundary conditions.*

Proof. Again we consider (61), (62) and (63). As before, at inner points we obtain the estimate (64). From (59), (62) and (63), substituting $\frac{\sigma_1^2}{h_1} \widehat{g}'_{1_{N_1, j}} = \frac{\sigma_1^2}{h_1} \widehat{u}_{\hat{x}_{1_{N_1, j}}}$, $\left(\frac{\sigma_1^2}{h_1} + \frac{\sigma_1^2}{h_2} \right) \widehat{g}'_{1_{N_1, N_2}} = \frac{\sigma_1^2}{h_1} \widehat{u}_{\hat{x}_{1_{N_1, N_2}}} + \frac{\sigma_1^2}{h_2} \widehat{u}_{\hat{x}_{2_{N_1, N_2}}}$ in view of (32) and (34), we get

$$\begin{aligned}
\|\widehat{u}\| & \leq \frac{1}{1+r\Delta\tau} \|u\| + \Delta\tau A_1^+ \|\widehat{g}'_1\|, \\
\|\widehat{u}\| & \leq \frac{1}{1+r\Delta\tau} \|u\| + \Delta\tau (A_1^+ + A_2^+) \|\widehat{g}'_1\|.
\end{aligned}$$

Then, taking into account also the Dirichlet boundary conditions (if any), the time integration procedure in general case leads to

$$\|u\| \leq \max\{\|g'_0\| + C \max_{\partial\Omega'_1} g'_1, T \max_{\partial\Omega'_2} g'_2\}, \quad \text{where } C = T(|A_1| + |A_2|). \tag{66}$$

5 Numerical Examples

In this section we test the accuracy, convergence rate and positivity preserving of the presented numerical methods for model problem (10)-(14) (and (4)-(8)). Model parameters are $D_1 = 0.0487902$, $D_2 = 0$, $\sigma_1 = \sigma_2 = 0.2$, $r = 0.0953102$ [22]. In agreement with (44) we can choose $h = h_1 = h_2$ ($N = N_1 = N_2$).

When we deal with exact solution (Example 1), the convergence rate in maximal discrete norm is computed using two consecutive meshes:

$$CR_\infty = \log_2 \frac{E_\infty^{N/2}}{E_\infty^N}, \quad E_\infty^N = \max_{1 \leq i, j \leq N_1} |E_{i,j}^N|,$$

where $E_{i,j}^N$ is the difference between the exact and the numerical solutions at point (x_{1_i}, x_{2_j}, T) on a mesh with $N \times N$ grid nodes in space.

Alternatively, if the exact solution is not available (Example 2), the convergence rate is computed by the same formula but now $E_{i,j}^N$ is the difference between two *numerical* solutions, computed on meshes with N and $2N$ grid nodes respectively.

In order to avoid division by zero in uniform flow regions, we add $\varepsilon \ll 1$ ($\varepsilon = 10^{-30}$) to both numerator and denominator of the gradient ratio (23).

Example 1 (Exact solution test) In the right hand side of the equation (10) we add an appropriate residual function and consider non-homogeneous Neumann boundary conditions on East, North and South boundary ($\partial\Omega'_1 \equiv \partial\Omega'_E \cup \partial\Omega'_N \cup \partial\Omega'_S$) and Dirichlet boundary conditions on the West boundary ($\partial\Omega'_2 \equiv \partial\Omega'_W$) such that

$$u(x_1, x_2, \tau) = e^{-\tau/2} \cos(\pi x_1/3) \cos(\pi x_2/3),$$

is the exact solution of the modified problem (10)-(14). The computations are performed in two domains:

$$\overline{\Omega}'^A = [-1, 1] \times [-1, 1], \quad \overline{\Omega}'^B \simeq [-\ln(200), \ln(200)] \times [-\ln(200), \ln(200)].$$

for $T = 0.5$ and fixed for all time levels time step $\Delta\tau = h^2$. The results for different values of ρ_1, ρ_2 in each domain $\overline{\Omega}'^A$ and $\overline{\Omega}'^B$ are given in Table 1. We observe second-order convergence rate of the numerical method.

Example 2 (Original problem) We solve (10)-(14) (and (4)-(8)) by the presented numerical method for different initial and boundary conditions. All computations are performed in $\overline{\Omega}'^B$ for $\rho_1 = -0.2$, $\rho_2 = 0.6$. For the convergence test we take $\Delta\tau = h^2$ fixed and $T = 2$, while the given plots are for different time and time steps, satisfying equality in (60). We denote by E the exercise price, w_i is the weight of the i -th asset, 'cap' parameter is used for capped-style options, BS (Price, Strike, Time) is the Black-Scholes vanilla Put/Call option price.

We consider the following test problems:

TP1: *European exchange option with pay-off*: $P(S_1, S_2) = \max\{0, S_2 - S_1\}$. We use the pay-off function as the source for the Dirichlet condition [11]. Namely, $\partial\Omega'_1 \equiv \emptyset$ and $g_2(S_1, S_2, t) = P(S_1, S_2)$.

TP2: *Worst-off two Call option with barrier* [29]. Now $P(S_1, S_2) = \max\{0, \min\{S_1, S_2\} - E\}$ and $\partial\Omega'_1 \equiv \emptyset$, $g_2(S_1, S_2, t) = P(S_1, S_2)$.

Table 1: Errors and convergence rates, Example 1

N	$\overline{\Omega}^A$		$\overline{\Omega}^B$			
	$\rho_1 = -0.2, \rho_2 = 0.6$		$\rho_1 = -1, \rho_2 = 1$			
	E_∞^N	CR_∞	E_∞^N	CR_∞	E_∞^N	CR_∞
21	6.48015e-4		1.69489e-2		1.69709e-2	
41	1.58029e-4	2.0359	4.83743e-3	1.8089	4.84391e-3	1.8088
81	3.83190e-5	2.0441	1.21792e-3	1.9898	1.21971e-3	1.9896
161	9.38348e-6	2.0299	2.86828e-4	2.0862	2.87575e-4	2.0845
321	2.32268e-6	2.0143	6.84829e-5	2.0664	6.86652e-5	2.0663

TP3: *Capped Put on a basket of two equities* [21, 22]. The initial function is $g_0 = \min\{\text{cap}, \max\{0, E - w_1 S_1 - w_2 S_2\}\}$, boundary conditions are (8) ($\partial\Omega'_1 \equiv \emptyset$) with

$$g_2 = \begin{cases} 0 & \text{on } \partial\Omega_N \cup \partial\Omega_E, \\ BS(S_1, \frac{E}{w_1}, t) - BS(S_1, \text{cap}, t) & \text{on } \partial\Omega_S, \\ BS(S_2, \frac{E}{w_2}, t) - BS(S_2, \text{cap}, t) & \text{on } \partial\Omega_W, \end{cases}$$

The boundary conditions at $\partial\Omega_W$ and $\partial\Omega_S$ represents the prices of capped European option with strike prices of E/w_1 and E/w_2 , respectively [22].

TP4: *Two-asset barrier options* [8, 22]. We consider $\partial\Omega'_1 \equiv \partial\Omega'_E \cup \partial\Omega'_N \cup \partial\Omega'_S$, $\partial\Omega'_2 \equiv \partial\Omega'_W$, $g_0 = \max\{0, w_1 S_1 - E\}$, $g_2 = 0$, $g_1 = 0$ on $\Omega_S \cup \Omega_N$, $g_1 = 1$ on Ω_E .

TP5: *Capped Call on a Basket of two equities* [21, 22]. In this case $\partial\Omega'_1 \equiv \partial\Omega'_E \cup \partial\Omega'_N$, $\partial\Omega'_2 \equiv \partial\Omega'_W \cup \partial\Omega'_S$, $g_0 = \min\{\text{cap}, \max\{0, w_1 S_1 + w_2 S_2 - E\}\}$, $g_1 = 0$ on $\Omega_N \cup \Omega_E$ and

$$g_2 = \begin{cases} BS(S_1, \text{cap}, t) - BS(S_1, \frac{E}{w_1}, t) & \text{on } \partial\Omega_S, \\ BS(S_2, \text{cap}, t) - BS(S_2, \frac{E}{w_2}, t) & \text{on } \partial\Omega_W, \end{cases}$$

In Table 2 we give convergence rate (CR_∞), computed on three consecutive meshes, for each test problem, $E = 100$, $w_1 = w_2 = 1$, $\text{cap} = 10$. We observe that the order of convergence

Table 2: Convergence rates for different problems, $\Delta\tau = h^2$, $T = 2$, Example 2

space meshes	TP1	TP2	TP3	TP4	TP5
21-41-81	1.4458	1.3809	0.7447	1.1625	0.7443
41-81-161	1.8038	1.5757	1.4963	1.4525	1.4732
81-161-321	2.0477	1.7639	1.8234	1.8884	1.8022

very close to 2 for all problems TP1-TP5.

Conclusions

In this paper we develop second-order in space implicit-explicit finite difference method, based on the van Leer flux-limiter technique, for the worst-case pricing model in financial mathematics. Under mild time and space step restrictions the proposed method is stable (with respect to initial and boundary conditions) and preserves the non-negativity of the numerical solution. Van Leer's flux limiter technique is implemented appropriately also for non-homogeneous Neumann boundary conditions, ensuring second order convergence rate and possibility to guarantee the positivity preserving property of the numerical solution.

Various numerical examples confirm the theoretical statements and illustrate the second order convergence in space variable.

The very important question - to find interface curve (in the one dimensional case) or surface (in the two-dimensional case) where the sign of Γ_{cross} changes and on this base to construct numerical method for the corresponding linear problems on both sides of the interface will be the main subject of our next work.

Acknowledgement

This research was supported by the European Union under Grant Agreement number 304617 (FP7 Marie Curie Action Project Multi-ITN STRIKE - Novel Methods in Computational Finance) and Bulgarian National Fund of Science under Project DID 02/37-2009.

References

- [1] M. Avellaneda, A. Levy, A. Parás, Pricing and hedging derivative securities in markets with uncertain volatilities, *Appl. Math. Fin.* 2 (1995) 73–88.
- [2] F. Black, M. Scholes, The pricing of options and corporate liabilities, *J.Pol. Econ.* 81 (1973) 637 – 659.
- [3] R. Company, L. Jódar, M. Fakharany, M.-C. Casabán, Removing the Correlation Term in Option Pricing Heston Model: Numerical Analysis and Computing, *Abstract and Applied Analysis* 2013 (2013) Article ID 246724, 11 pages
- [4] Ehrhardt, M. (Ed) *Nonlinear Models in Mathematical Finance: New Research Trends in Option Pricing*, Nova Science Publishers, N.Y. (2008).
- [5] L. C. Evans, *Partial Differential Equations*, 2nd edition, American Math Society, 2010.
- [6] A. Gerisch, D.F. Griffiths, R. Weiner, and M.A.J. Chaplain, A Positive splitting method for mixed hyperbolic-parabolic systems, *Num. Meth. for PDEs* 17(2) (2001), 152–168.
- [7] Z. Horváth, Positivity of Runge-Kutta and diagonally split Runge-Kutta methods, *Appl. Numer. Math.* 28 (1998), 309–326.
- [8] E. G. Haug, *The Complete Guide to Option Pricing Formulas*, New York, 1997.
- [9] W. Hundsdorfer, *Numerical Solution of Advection-Diffusion-Reaction Equations*, Lecture Notes, Thomas Steiljes Inst. CWI Amstrdam, 2000.

- [10] W. Hundsdorfer, J. Verwer, Numerical Solution of Time-Dependent Advection-Diffusion-Reaction Equations, Springer Series in Computational Mathematics 33, Springer-Verlag, Berlin, Heidelberg, New York, 2003.
- [11] R. Kangro, R. Nicolaides, Far field boundary condition for Black-Scholes equations, SIAM J. Numer. Anal. 38(4) (2000) 1357–1368.
- [12] M. Koleva, Positivity preserving numerical method for non-linear Black-Scholes models, Lect. Notes Comp. Sci. 8236 (2013) 363–370.
- [13] D. Kusmin, S. Turek, High-resolution FEM-TVD schemes based on a fully multidimensional flux limiter, J. Comp. Phys. 198(1) (2004), 131–158.
- [14] B. van Leer, Towards the ultimate conservative difference scheme II. Monotonicity and conservation combined in a second order scheme, J. Comput. Phys. 14 (1974), 361–370.
- [15] R.J. LeVeque, Numerical Methods for Conservation Laws, Birkhäuser, 1992.
- [16] Jun Ma, A stochastic correlation model with mean revision for pricing multi asset options, Asia-Pacific Finan. Markets 16 (2009) 97 – 109.
- [17] D.M. Pooley, P.A. Forsyth, K.R. Vetzal, Numerical convergence properties of option pricing PDEs with uncertain volatility, IMA J. Numer. Anal. 23 (2003) 241–267.
- [18] I.V. Rybak, Monotone and conservative difference scheme for elliptic equations with mixed derivatives, Math. Model. and Anal. 9(2) (2004) 169–178.
- [19] Samarskii A. A., The Theory of Difference Schemes, Marcel Dekker Inc, 2001.
- [20] A. Samarskii, V. Mazhukin, P. Matus and G. Shishkin, Monotone difference schemes for equations with mixed derivatives, Mathematical Modeling 13(2) (2001) 17–26, 2001
- [21] J. Topper, Finite element modeling of exotic options, Discussion paper 216, Universität Hannonver, 1998.
- [22] J. Topper, Worst case pricing of rainbow options. Discussion paper 217, Fachbereich Wirtschaftswissenschaften, Universität Hannonver, October 2001 (ISSN 0949-9962).
- [23] J. Topper, Uncertain parameters and reverse convertibles, Risk 14 (2001) 1-14.
- [24] J. Topper, Financial Engineering with Finite Elements, Chapter 10, p.248, Wiley, 2005, 360p.
- [25] Tavella, D., Randall, C. *Pricing Financial instruments*, Wiley, New York (2000).
- [26] R.S. Varga, Matrix Iterative Analysis, Springer-Verlag Berlin Heidelberg, 2000 (Second Revised and Expanded Edition).
- [27] P. Wilmott, Derivatives: The Theory and Practice of Financial Engineering, Chapter 27, pages 383–393, Wiley, 1998.
- [28] H. Windcliff, J. Wang, P.A. Forsyth, K.R. Vetzal, Hedging with a Correlated Asset: Solution of a Nonlinear Pricing PDE, J. of Comp. and Appl. Math. 200 (2007) 86–115

- [29] R. Zvan, K.R. Vetzal, P.A. Forsyth, PDE methods for pricing barrier options, *J. of Economics Dynamics & Control* 24 (2000) 1563–1590.